

Nighttime Person Re-Identification via Collaborative Enhancement Network with Multi-domain Learning

Andong Lu Tianrui Zha Chenglong Li Jin Tang Xiaofeng Wang Bin Luo

Anhui Provincial Key Laboratory of Multimodal Cognitive Computation
School of Computer Science and Technology, Anhui University, Hefei, China
School of Artificial Intelligence, Anhui University, Hefei, China
School of Computer Science and Technology, Hefei University, Hefei, China

Abstract

Prevalent nighttime ReID methods typically combine relighting networks and ReID networks in a sequential manner, which not only restricts the ReID performance by the quality of relighting images, but also neglects the effective collaborative modeling between image relighting and person ReID tasks. To handle these problems, we propose a novel Collaborative Enhancement Network called CENet, which performs the multilevel feature interactions in a parallel framework, for nighttime person ReID. In particular, CENet is a parallel Transformer network, in which the designed parallel structure can avoid the impact of the quality of relighting images on ReID performance. To perform effective collaborative modeling between image relighting and person ReID tasks, we integrate the multilevel feature interactions in CENet. Specifically, we share the Transformer encoder to build the low-level feature interaction, and then perform the feature distillation to transfer the high-level features from image relighting to ReID. In addition, the sizes of existing real-world nighttime person ReID datasets are small, and large-scale synthetic ones exhibit substantial domain gaps with real-world data. To leverage both small-scale real-world and large-scale synthetic training data, we develop a multi-domain learning algorithm, which alternately utilizes both kinds of data to reduce the inter-domain difference in the training of CENet. Extensive experiments on two real nighttime datasets, Night600 and RGBNT201_{r,gb}, and a synthetic nighttime ReID dataset are conducted to validate the effectiveness of CENet. We will release the code and synthetic dataset.

1. Introduction

Person re-identification (ReID) is the task of identifying individuals in the images captured by different surveillance cameras, and it has significant potential applications in the fields of public security and criminal investigations. Despite current state-of-the-art methods [2, 7, 9, 19, 31, 33–35] achieve excellent performance in ReID during the daytime, the challenges of re-identifying person in nighttime scenarios remains unsolved. The main reason can be attributed to the severe image degradation and reduced visibility of nighttime person images. Hence, a straightforward approach to address the nighttime person ReID problem commonly involves the application of a relighting technique to enhance the visibility of input images before feeding them into the ReID network, as illustrated in Figure 1 (a). However, this method is not always effective since the conventional relighting technique is not specifically tailored to the ReID task.

To overcome this limitation, existing works [18, 36] propose end-to-end nighttime person ReID methods that integrate relighting and ReID within a single framework, as depicted in Figure 1 (b). For instance, Zhang et al. [36] propose an end-to-end network that optimizes both the denoising and ReID objectives, leading to effective performance improvement compared to baseline methods. Nevertheless, their approach overlooks the challenges posed by low-light conditions in nighttime images. Lu et al. [18] propose an illumination distillation network that combines features from nighttime images and relighting images. This method aims to mitigate the limitations of solely relying on relighting images. Although these methods demonstrate promising performance improvements, they still follow a sequential approach of integrating relighting and ReID networks. Consequently, the performance of the ReID network is not only constrained by the quality of the relight-

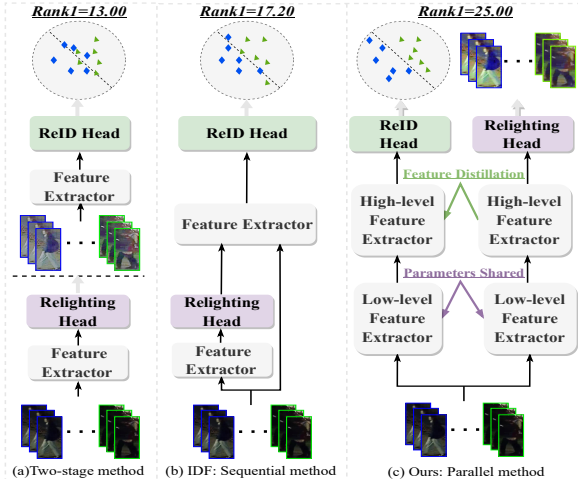


Figure 1. Comparison of three nighttime person ReID strategies. (a) uses Zero.DCE [8] for low-light image pre-processing and TransReID [9] for recognition. (b) represents the current state-of-the-art sequential end-to-end nighttime ReID method IDF [18]. (c) introduces our proposed parallel end-to-end method, which outperforms the other strategies. Evaluation is performed on the nighttime ReID dataset *Night600* [18].

ing image, but also lacks collaborative modeling between in two networks. Moreover, most existing relighting networks [8, 15, 37] simply stack multiple convolutional layers, making it challenging to capture the crucial global context necessary for modeling lighting variations.

To address these challenges, we introduce the Collaborative Enhancement Network (CENet) that integrates ReID and relighting networks in parallel, as depicted in Figure 1 (c). This parallel structure design mitigates the impact of relighting image quality on the ReID model, and the designed multi-level feature interaction achieves effective collaborative modeling in ReID and re-illumination networks. CENet comprises three primary components: a shared encoder, a relighting subnet, and a ReID subnet. These components collaborate to learn lighting-enhanced features for both relighting and ReID tasks. Benefiting from relighting task-driven, the shared encoder can extract lighting-enhanced features from nighttime images, which helps to enhance the low-level ReID feature. Furthermore, feature distillation scheme distills lighting information from the decoder features of the relighting subnet to guide feature learning in the ReID subnet.

In the existing real nighttime dataset, we encounter challenges when training the proposed network due to its limited scale and the relighting network is hard to obtain corresponding daytime images for learning. To this end, we synthesize a large-scale nighttime dataset called *Syn_Dark*, which is created by introducing random factors, including illumination, color, and contrast variations, into two ReID datasets, *Market1501* [42] and *MSMT17* [28]. However, solely relying on synthesized data limits the network’s per-

formance on real-world nighttime ReID datasets. To overcome this limitation, we design a multi-domain learning approach that combines both real and synthesized data domains. Our approach learning the network in the real domain using an unsupervised relighting method based on the *RetineX* theory. Simultaneously, in the synthetic domain data, which includes pairs of daytime ground-truth images, we employ a fully supervised method. During the iterative training process, we alternate between different domains and their respective learning approaches to comprehensively optimize the entire network. This strategy helps reduce the domain gap and improve the network’s performance on real-world nighttime ReID datasets.

In summary, the main contributions are as follows:

- We propose a new parallel framework that addresses the impact of relighting image quality on the ReID task. Furthermore, our framework can get rid of relighting subnet during test time, avoiding additional inference costs.
- We design an novel multilevel feature interaction strategy to facilitate collaborative modeling between the ReID and relighting networks, which enhances the ReID network’s feature representation capability specifically for nighttime images.
- We present an efficient multi-domain learning strategy that effectively utilizes large-scale synthetic data to overcome the limitations of model training with small-scale real night data.

2. Related Work

2.1. Nighttime Person ReID Methods

Due to the challenges posed by low-light conditions at night, visible light cameras often struggle to capture clear images during nighttime. Some studies [20, 29] propose to use visible light devices during the day and introduce infrared devices at night to capture person images, named cross-modality person ReID. Recently, research in this field has attracted increasing attention [16, 25, 30, 32, 33, 39], with the primary challenge is reducing the differences between various modalities. To address this, Li et al.[16] employ a self-supervised learning network by establishing an intermediate X modality to mitigate the modalities gap. Zhang et al.[39] develop a network that improves the consistency of features across different channels. Ye et al.[30] propose a strategy involving random color channel swapping to create images that are not dependent on color within the same modality. Other studies [10, 11, 40] synthesize low-light datasets to explore challenges of low-light images, which ignores synthetic data hard to reflect the real challenges of person ReID at night. To this end, Zhang et al. [36] introduce a nighttime person ReID dataset focusing on the noise of nighttime images, and propose a denoising-then-match framework. Then, Lu et al. [18] propose a

real nighttime ReID dataset that considers complex lighting conditions and develops an enhancement-then-match framework. However, these methods are still constrained by the quality of relighting images. This paper presents a parallel architecture integrating relighting and ReID networks, which effectively avoids direct dependence on relighting images, and designs a multi-level feature enhancement scheme between the two networks.

2.2. Relighting Methods

The relighting task aims to recover invisible regions in low-light images. Some classic methods [5, 12–14, 21, 22] adjust image brightness by different theories and provides an important foundation for future research. With the rise of deep learning, a series of methods combine convolutional neural networks and *RetineX* theory [27, 37, 38] to achieve more accurate enhancement effects. Wei et al. [27] first used *RetineX* theory with a deep neural network, employing a two-step approach of image decomposition followed by enhancement. Zhang et al. [38] design a simple and effective network that maps the illumination and reflection maps to different subspaces, enabling separate correction of brightness and degradation. However, these methods heavily rely on paired data for training, limiting their applicability. To address this limitation, Guo et al. [8, 15] design a network to generate pixel-level curve parameter maps, which are then used to adjust low-light images. Zhang et al. [37] propose an unsupervised relighting network based on information entropy and *RetineX* theory, which only uses low-light images for learning and outputs light and reflection maps. However, pretrained relighting networks cannot guarantee the optimal performance for person ReID tasks at night.

3. Methodology

In this section, we introduce the proposed collaborative enhancement network in detail, including network overview, ReID branch, relighting branch, multilevel feature interactions, and multi-domain joint learning scheme.

3.1. Network Overview

The proposed network framework, as illustrated in Figure 2, comprises three main components: the shared encoder, ReID subnet, and relighting subnet. By combining the shared encoder with the ReID subnet and relighting subnet, we establish the ReID branch and relighting branch, enabling a parallel architecture for both vision tasks. To elaborate, we first utilize the shared encoder to extract features from nighttime person images. These features are then directed to two distinct task subnets, each producing its respective output results. The design of the shared encoder allows the ReID task to benefit from the low-level features relevant to the relighting task. In addition, we introduce a feature distillation mechanism to enhance the high-level

feature representation in the ReID subnet. In contrast to existing methods, our proposed network achieves effective collaborative modeling between image relighting and ReID tasks, while avoiding the impact of enhanced image quality on ReID performance.

3.2. ReID Branch

Feature Extraction. The ReID branch adopts the Transformer network ViT [6] with strong representation ability as the feature extraction network. Within this branch, the initial 5 encoders are designated as the shared encoder, while the remaining 6 encoders and task head serve as the ReID subnet. We partition the nighttime image X into N equally-sized image patches denoted as $X_p^i | i = 1, 2, \dots, n$, incorporating a trainable global token X_{cls} as the input sequence for the ReID branch. Additionally, drawing from the TransReID [9], we incorporate a learnable position embedding into the input sequence. Moreover, we introduce camera information embedding to enhance the acquisition of invariant features within the input sequences. Subsequently, the input sequence is passed to the shared encoder, yielding the shared features, which can be expressed as:

$$F_{share} = [\mathcal{E}(x_{cls}); \mathcal{E}(x_p^1); \mathcal{E}(x_p^2); \dots; \mathcal{E}(x_p^N)] \quad (1)$$

where \mathcal{E} represents the shared encoder, and F_{share} corresponds to the output features produced by the shared encoder. Given that ReID is a classification task, extracting deep high-level semantic features is essential for distinguishing target individuals. To achieve this, we establish a ReID subnet comprising 6 Transformer encoders to extract more discriminative identity features. Finally, we employ a fully connected layer to adjust the number of extracted identity features for the final classification.

Task Learning. We employ triplet loss and identity loss for joint optimization. In specific, the identity loss is the cross-entropy loss without label smoothing, which can be formulated as:

$$\mathcal{L}_{ID} = -\frac{1}{B} \sum_{i=1}^B \sum_{j=1}^N y_{i,j} \log\left(\frac{e^{\alpha(s_{i,j}-m)}}{e^{\alpha(s_{i,j}-m)} + \sum_{k \neq j} e^{\alpha s_{i,k}}}\right) \quad (2)$$

where B and N represent the total number of samples and identities, respectively. Additionally, $y_{i,j}$ denotes the label assigned to the j -th identity of the i -th sample, while $s_{i,j}$ represents the score assigned to the j -th identity of the i -th sample. The variable m represents the mean value of the identity score, and α is the temperature parameter. The triplet loss is defined as follows:

$$L_{Tri} = \max(0, \alpha + d(f_a, f_p) - d(f_a, f_n)) \quad (3)$$

where f_a , f_p , and f_n denote the feature representations of anchor samples, positive samples, and negative samples, respectively. Here, d denotes the Euclidean distance, and α

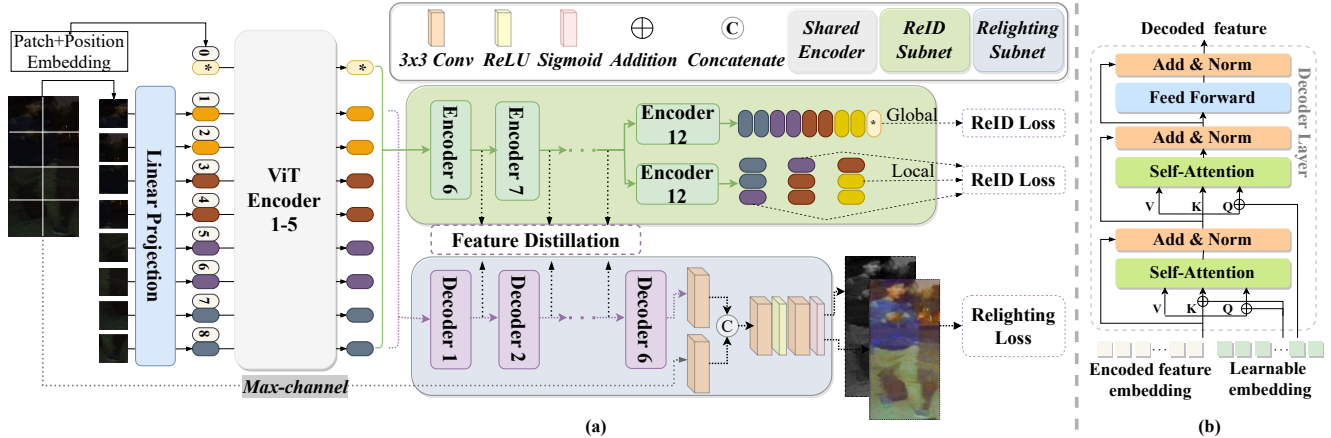


Figure 2. (a) The architecture of the collaborative enhancement network for nighttime ReID. (b) The detail of the transformer decoder, where \oplus represents the feature addition.

is a constant value used to control the feature margin. Furthermore, we optimize the ReID branch from both global and local perspectives, aiming to learn more fine-grained information. More detailed information in [9].

3.3. Relighting Branch

As shown in Figure 2 (a), the relighting branch comprises a shared encoder and a relighting subnet. Considering that image relighting is an image reconstruction task rather than a classification task, we exclude the X_{cls} component from F_{share} and denote it as F_{share}^* . Subsequently, we forward it to the relighting subnet to perform image relighting.

Relighting Subnet. The relighting branch incorporates 6 Transformer decoders to decode the shared features F_{share}^* and utilize them for subsequent image reconstruction. These decoders consist of multi-head self-attention modules and feedforward networks. Within each decoder layer, the attention calculation is performed using the global representation F_{share}^* and the task-specific learnable embedding T_e as inputs, as illustrated in Figure 2 (b). The output features of the decoder are further processed through a sequence of convolutional layers, combined with the maximum channel of the input image, to generate a reflectance map (relighting result) of the input image and a corresponding lighting map. Specifically, the output features of the decoder and the maximum channel of the input image undergo separate 3×3 convolutional operations for refinement. Subsequently, they are concatenated along the channel dimension and passed through two additional convolutional layers with activation functions to enable comprehensive fusion, resulting in a 4-channel image. Finally, the *Sigmoid* function is applied to constrain these results. The first three channels represent reflection maps, while the last channel corresponds to the lighting map.

3.4. Multilevel Feature Interactions

To improve ReID performance in low-light night scenes, we abandon the conventional approach [4, 18, 36] of extracting ReID features from relighting images. Instead, we focus on enhancing ReID feature representation from collaborative modeling between two tasks. Specifically, we adopt two strategies to achieve the enhancement from the relighting branch to the ReID branch. Since low-level networks typically capture common image features, we utilize parameter-sharing scheme between the ReID and relighting branches to improve low-level feature representation. Considering different tasks within high-level networks often model task-specific knowledge, which poses challenges for direct interaction. To this end, we propose a feature distillation strategy to enhance high-level feature in the ReID branch.

Shared Encoder. The shared encoder is designed to extract crucial information from input nighttime images, serving both the joint learning ReID task and the relighting task. Unlike traditional convolutional neural networks with limited receptive fields, we equip this extractor with ViT encoders [6], which allows for better capturing of global information within nighttime images. Moreover, the extractor excludes downsampling operations, thus preserving the spatial structure and detailed information in shallower layers. This preservation is particularly advantageous for the image relighting process. Therefore, benefiting from the learning of the relighting task, the shared encoder will share the ability to extract lighting-enhanced features in both tasks.

Feature Distillation. High-level networks tend to model task-specific knowledge in various tasks. Therefore, it is a challenging problem to leverage the high-level features of the relighting subnet to enhance the high-level features of the ReID subnet. To address this issue, we adopt a non-intrusive interactive strategy known as feature distillation to enhance ReID features. By analyzing the correlation between the two tasks, we introduce a content-independent

brightness loss to assist the ReID subnet. However, this overall brightness enhancement might amplify the brightness differences in person captured from various viewpoints. Consequently, we also incorporate a feature contrastive loss to ensure consistent feature representation for person from the same class, even under different lighting conditions. Finally, based on the above losses, we propose a novel lighting distillation loss to achieve high-level feature interaction between relighting and ReID tasks and improve the performance of the ReID task. Specifically, the lighting distillation loss can be formulated as:

$$L_{LD} = \underbrace{\|\varphi(f_s), \varphi(f_t)\|_2}_{\text{brightness loss}} - \log\left(\frac{\exp(\text{sim}(f_s, f_t))}{\frac{1}{N} \sum_{i=1}^N \exp(\text{sim}(f_s, f_t^i))}\right)$$

contrastive loss

where $\varphi()$ represents the feature channel mean function, and $\|\cdot\|_2$ denotes a mean square function. N is the number of samples in the dataset, $\text{sim}(u, v)$ denotes a similarity measure between u and v , and i and j are indices of data points, indicating whether x_i and x_j are samples from the same class or different classes.

3.5. Multi Domain Learning

To overcome the challenge of the small size of existing nighttime ReID dataset, we synthesize a large-scale nighttime person ReID dataset by applying multi-dimensional random degradation to existing daytime person ReID datasets (*Market1501* [42] and *MSMT17* [28]). Specifically, we apply lighting, contrast, color, and hue as four degradation factors to daytime images, generating diverse nighttime images that correspond to real nighttime scenarios, as depicted in Figure 3. However, there are large inter-domain

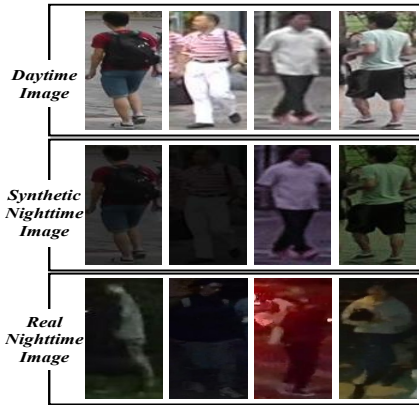


Figure 3. Comparison of real and synthetic domain data samples differences between synthetic data and real nighttime data. To tackle this challenge, this study introduces a novel multi-domain learning scheme, illustrated in Figure 4. Within this scheme, the ReID branch performs shared learning in the two domains, effectively enhancing its learning of domain-

invariant knowledge. The learning process of the entire network alternates between the two domains, employing supervised relighting learning in the synthetic domain and unsupervised relighting learning in the real domain. In the following sections, we will provide a detailed explanation of the learning approaches adopted in both domains.

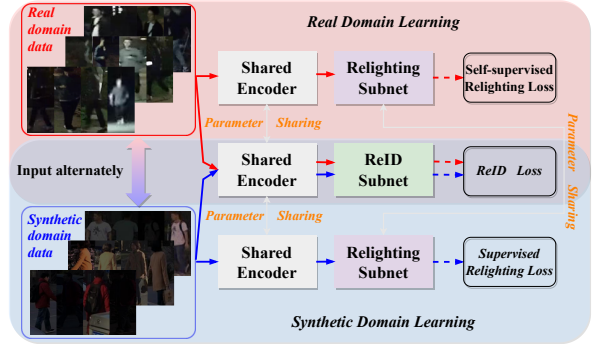


Figure 4. The overview of the proposed multi-domain learning.

Synthetic Domain Learning: In this stage, we establish a supervised low-light image relighting scheme utilizing synthetic low-light data and their corresponding well-lit counterparts. Given access to the corresponding ground truth, we employ the Euclidean distance as the loss function for this scheme, denoted as \mathcal{L}_{IE_s} , which can be expressed as:

$$\mathcal{L}_{IE_s} = \frac{1}{N} \sum_{i=1}^N \|I_{L_i} - I_{H_i}\|_2^2 \quad (4)$$

where N represents the total number of training samples, I_{L_i} and I_{H_i} denote the synthetic low-light image and corresponding well-lit image, respectively. $\|\cdot\|_2$ indicates the Euclidean distance between two images. This loss function quantifies the discrepancy between the synthetic low-light image and its corresponding well-lit image, with the objective of minimizing this difference during training.

To facilitate joint optimization with the ReID branch, we introduce a hyperparameter λ_1 to balance the weights of the two loss functions. Consequently, the overall loss function at this stage can be expressed as:

$$\mathcal{L}_{Syn} = \mathcal{L}_{ID} + \mathcal{L}_{Tri} + \lambda_1 \mathcal{L}_{IE_s} + \lambda_2 \mathcal{L}_{lig} \quad (5)$$

where $\lambda_1 = 0.5$ and $\lambda_2 = 0.1$ serves as hyperparameters that control the weight of the relighting loss.

Real Domain Learning. Given the challenges of obtaining highly corresponding low-light person images at night and well-lit person images during the day in real-world scenes, we adopt an unsupervised relighting learning strategy to enhance low-light images. Specifically, we employ the *RetineX* model to decompose an image as follows:

$$\mathcal{M} = \mathcal{R} \times \mathcal{I}. \quad (6)$$

The *RetineX* model provides a framework for separating the reflectance and lighting components in an image. In this case, the visible light image \mathcal{M} is decomposed into the reflectance map \mathcal{R} , which captures the inherent characteristics of the scene, and the lighting map \mathcal{I} , representing the varying lighting conditions.

Relighting in unsupervised scenarios presents a highly ill-posed problem. To address this issue, we draw inspiration from [37] and incorporate essential prior information along with four loss functions: (1) reconstruction loss \mathcal{L}_{rec} , (2) reflection loss \mathcal{L}_{ref} , (3) Color loss \mathcal{L}_{col} (4) structure-aware smoothing loss \mathcal{L}_{sa} .

First, we utilize the reconstruction loss (\mathcal{L}_{rec}) to preserve the invariance of image content and structural information. In this study, we employ a combination of mean absolute error loss and structural similarity loss for jointly constrain:

$$\mathcal{L}_{rec} = 1 - SSIM(\mathcal{R} \cdot \mathcal{I}, \mathcal{M}) + \|\mathcal{R} \cdot \mathcal{I} - \mathcal{M}\|_1 \quad (7)$$

where $SSIM(u, v)$ and $\|\cdot\|$ represent the structural similarity index and L1 norm, respectively.

Second, in low-light image relighting tasks, it is crucial to preserve maximum entropy in the enhanced image while maintaining consistency with the input image information. Specifically, the reflection map \mathcal{R} is defined as the element-wise division of \mathcal{M} by \mathcal{I} . Consequently, errors in estimating the lighting map can have exponential effects on the quality of the reflected image. To promote smoothness in the reflection map, a commonly employed regularization constraint is introduced:

$$|\Delta\mathcal{R}| = |\nabla_x \mathcal{R}| + |\nabla_y \mathcal{R}| \quad (8)$$

$\Delta\mathcal{R}$ represents the difference between neighboring pixels in the reflection map, while ∇_x and ∇_y denote the gradients in the horizontal and vertical directions, respectively. Thus, the overall reflection loss can be defined as follows:

$$\mathcal{L}_{ref} = \left\| \max_{c \in \{r, g, b\}} R^c - \mathcal{H} \left(\max_{c \in \{r, g, b\}} M^c \right) \right\|_1 + \|\Delta\mathcal{R}\|_1 \quad (9)$$

where $\mathcal{H}()$ denotes histogram equalization applied to the image, and $\max_{c \in \{r, g, b\}}$ selects the channel with the maximum pixel value in the image.

Third, a color loss is introduced to control the color shift problem during the enhancement process using the Gray-world color constancy hypothesis [3], which can be described as follows:

$$\mathcal{L}_{col} = \sum_{\forall (i, j) \in \varepsilon} (R^i - R^j)^2, \varepsilon = \{(r, g), (r, b), (g, b)\}. \quad (10)$$

where C^i indicates the average intensity value of the i -th channel of the lighting-enhanced image.

Finally, a structure-aware smoothing loss [27] is applied to constrain the reconstruction of enhanced images:

$$\mathcal{L}_{sa} = \|\Delta\mathcal{I} \cdot \exp(-\Delta\mathcal{R})\|_1. \quad (11)$$

This loss essentially weights the original TV function [1] ($\|\Delta\mathcal{I}\|_1$) by the gradient of reflectance.

Hence, the unsupervised relighting loss function is defined as follows:

$$\mathcal{L}_{IE_r} = \lambda_a \mathcal{L}_{rec} + \lambda_b \mathcal{L}_{ref} + \lambda_c \mathcal{L}_{col} + \lambda_d \mathcal{L}_{sa}. \quad (12)$$

In this study, we set λ_a , λ_b , λ_c , and λ_d to 1, 0.1, 0.2, and 0.1, respectively. Finally, the overall learning loss function for real domain data is defined as:

$$\mathcal{L}_{Real} = \mathcal{L}_{ID} + \mathcal{L}_{Tri} + \lambda_1 \mathcal{L}_{IE_r} + \lambda_2 \mathcal{L}_{lig}. \quad (13)$$

Here, λ_1 and λ_2 are consistent with the settings of λ_1 and λ_2 setting in synthetic domain learning.

4. Experiment

In this section, we present an overview of our experimental setup and proceed to conduct a comprehensive evaluation and comparison of the proposed method on three datasets: two real nighttime ReID datasets and one synthetic ReID dataset. We follow the common evaluation protocol in the field of ReID. We employ two standard metrics: the Cumulative Matching Characteristic (CMC) curve and the mean Average Precision (mAP).

4.1. Experiment Settings

Implementation Details. In this paper, CENet utilizes the TransReID [9] network as the backbone in the ReID branch. The backbone is equipped with an *ImageNet* pre-trained model for feature extraction. Corresponding classification head networks are designed for both the real domain dataset and the synthetic domain dataset, tailored to their respective number of categories. In the relighting branch, the shared encoder follows the aforementioned parameters. However, the relighting subnet uses randomly initialized parameters, which allows the framework to learn specific features for low-light image relighting. The entire framework is trained end-to-end on the real domain dataset *Night600* and the synthetic domain dataset *Syn_Dark*. Specifically, all images are resized to a size of 256×128 , and random horizontal flipping, cropping, and random erasing techniques are applied during training to mitigate overfitting issues. Each batch size is set to 64, and the initial learning rate is set to 0.008. We employ stochastic gradient descent (SGD) optimizer with a momentum of 0.9 and weight decay of $1e-4$. *In testing phase, CENet can only perform the ReID branch, which gets rid of the extra computational cost of existing methods that rely on relighting results during inference.*

Dataset. For this study, we utilize the *Night600* dataset [18] as our real domain data. This dataset comprises a total of 28,813 nighttime images of 600 different person, captured by a total of 8 cameras, and divided into a training set and a test set. To create a synthetic nighttime ReID

dataset, we adjust the brightness, contrast, hue, and color parameter ranges of images from the *Market1501* [42] and *MSMT17* [28] datasets. We set the brightness parameter range between (10, 38) and the contrast parameter range between (7, 30) to reduce brightness and contrast. Additionally, the image hue and color parameter ranges are set to (7, 30) and (20, 35) respectively, simulating the common color imbalance challenges in nighttime scenes. Furthermore, we introduce a multi-modality ReID dataset called **RGBNT201** [41]. This dataset consists of three highly aligned modalities: RGB, near-infrared, and thermal infrared. It focuses on capturing low-light scenes at night. To evaluate the performance of unimodal ReID methods in nighttime scenes, we utilize only the RGB modality data from this dataset, denoted as **RGBNT201_{rgb}**. Table 1 pro-

Table 1. Statistics on real and synthetic domain datasets

Dataset	Train	Query	Gallery
<i>Night600</i>	300/14462	300/2180	300/14351
RGBNT201_{rgb}	171/3951	30/836	30/836
<i>Syn_Dark</i>	4852/138984	750/3368	750/13115

vides a detailed overview of the two real-world datasets and one synthetic dataset. The *Syn_Dark* dataset offers a greater number of unique identities and images compared to both the *Night600* and **RGBNT201_{rgb}** datasets. Subsequent experiments show that demonstrate that exposing the model to a wider range of identities and variations is crucial for training and improving performance.

4.2. Comparison with State of the Arts

In this section, we compare CENet with six state-of-the-art ReID algorithms: IDE+ [43], PCB [23], ABD-Net [2], AGW [31], BoT [19], and TransReID [9] on the *Night600*, **RGBNT201_{rgb}** and *Syn_Dark* datasets. To ensure fair evaluation, we retrain all methods using nighttime data. Additionally, we compare the proposed method (CENet) with IDF [18], which is a state-of-the-art ReID method designed for night scenes. As shown in Table 2, CENet demonstrates a significant performance advantage over all competing algorithms in real nighttime datasets. When compared to IDF on both the *Night600* and **RGBNT201_{rgb}** datasets, CENet achieves impressive improvements of 4.1% in mAP and 7.8% in Rank1, as well as substantial gains of 17.3% in mAP and 19.0% in Rank1, respectively.

Moreover, we evaluate CENet with state-of-the-art multi-modality ReID methods on the **RGBNT201** dataset. As shown in Table 3, CENet only relies on RGB modality data and achieves performance that significantly surpasses that of the state-of-the-art multi-modal ReID algorithms. Specifically, CENet outperforms IEEE [26] by a significant margin, achieving improvements of 8.9% in mAP and 10.3% in Rank-1 metrics, which indicates that visible light images at night also contain huge potential.

4.3. Ablation Study

In this section, we evaluate the effectiveness of each component in CENet on two different datasets: a real nighttime ReID dataset (*Night600*) and a synthetic ReID dataset (*Syn_Dark*). We systematically isolate and evaluate the three components within CENet: parameter sharing (PS), feature distillation (FD), and multi-domain learning (MD). Specifically, we first exclude MD from CENet, labeling it as "CENet w/o MD". As we can observe from Table 4, the exclusion of MD leads to a notable decline in performance. Subsequently, we individually exclude PS and FD, labeling them as "CENet w/o MD PS" and "CENet w/o MD FD". This also results in a degradation in model performance. Finally, we exclude all the components proposed in this paper, establishing it as the baseline method referred to as "CENet w/o MD FD PS". Further detailed results are presented in Table 4, which illustrates that each component plays an important role in nighttime person ReID.

To evaluate the effectiveness of the proposed lighting distillation (LD) loss, we also consider two commonly used feature distillation losses: mean squared error (MSE) loss and Kullback-Leibler (KL) loss for feature distillation. To this end, we construct three different variants, namely CENet-LIG w/o MD, CENet-MSE w/o MD, and CENet-KL w/o MD, which respectively indicate replacing LD with only lighting loss, MSE loss, and KL loss. From the results in Table 5, it can be observed that these variant losses do not bring performance improvement when applied to the real nighttime dataset *Night600*. This demonstrates the effectiveness of the proposed LD loss.

4.4. Visualization

We present the output results of the relighting branch based on the "CENet w/o MD" and the "CENet" in Figure 5. It can be observed that the "CENet w/o MD" effectively enhances the brightness of low-light images, indicating that increasing the brightness of nighttime images contributes to improved nighttime ReID performance. However, the unsupervised learning approach in the relighting branch exhibits limitations in terms of color shift and noise smoothing, as illustrated in the second row of Figure 5. In contrast, CENet incorporates a supervised relighting learning process using synthetic data. CENet not only improves the image brightness but also enhances the color quality and smoothness of noise, leading to better performance. This highlights the importance of enhancing the color and noise quality of nighttime images for nighttime ReID performance.

In addition, we randomly selected 12 different samples from the test set and extracted their features using three models: baseline, CENet w/o MD, and CENet. Then, we visualized the distribution of the sample features using t-SNE technique [24]. Figure 6 (a) shows the representation distribution of these sample features by the baseline model,

Table 2. Comparison results of CENet with state-of-the-art ReID methods on real and synthetic nighttime ReID datasets

Testing Dataset	<i>Night600</i> [18]				<i>RGBNT201_{rgb}</i> [41]				<i>Syn_Dark</i>			
	mAP	Rank-1	Rank-5	Rank-10	mAP	Rank-1	Rank-5	Rank-10	mAP	Rank-1	Rank-5	Rank-10
IDE+ [43]	3.38	7.75	20.09	27.43	19.44	17.23	30.38	37.44	68.31	87.50	95.67	97.33
PCB [23]	6.09	12.84	26.47	35.14	17.88	14.35	28.83	35.89	71.31	88.99	95.93	97.65
ABD-Net [2]	7.23	14.36	29.59	40.00	19.04	15.67	26.32	35.89	41.06	65.20	74.20	82.42
BoT [19]	5.40	11.20	22.60	30.60	21.90	19.30	32.80	43.50	56.10	81.00	92.30	94.90
AGW [31]	6.10	12.50	24.40	30.90	23.70	21.10	37.20	49.30	73.40	90.60	96.60	98.10
TransReID [9]	8.40	16.00	31.10	39.90	36.10	34.70	53.60	63.20	75.50	89.90	96.30	97.70
IDF [18]	9.20	17.20	34.40	43.80	38.00	38.40	53.70	63.20	75.10	88.70	95.50	97.20
CENet	13.30	25.00	43.00	51.70	55.30	57.40	73.60	81.50	79.20	91.70	97.00	98.20

Table 3. Comparison results of CENet with state-of-the-art multi-modality methods on *RGBNT201* dataset

Methods	Modality	mAP	Rank-1	Rank-5	Rank-10
HAMNet [17]		27.70	26.30	41.50	51.70
PFNet [41]	RGB+NI+TIR	38.50	38.90	52.00	58.40
IEEE [26]		46.40	47.10	58.50	64.20
CENet	RGB	55.30	57.40	73.60	81.50

Table 4. Ablation studies of CENet on *Night600* and *Syn_Dark* datasets

	<i>Night600</i>			<i>Syn_Dark</i>		
	mAP	Rank-1	Rank-5	mAP	Rank-1	Rank-5
CENet	13.30	25.00	43.00	79.20	91.70	97.00
CENet w/o MD	9.50	19.20	33.50	77.30	91.00	96.60
CENet w/o MD PS	8.80	16.10	31.30	79.80	91.90	97.20
CENet w/o MD FD	8.90	17.20	31.50	76.20	90.00	96.20
CENet w/o MD FD PS	8.40	16.00	31.10	75.50	89.90	96.30

Table 5. Lighting distillation (LD) loss ablation studies on the *Night600* dataset

Methods	mAP	Rank-1	Rank-5	Rank-10
CENet-LD w/o MD	9.50	19.20	33.50	41.90
CENet-LIG w/o MD	9.00	17.00	31.20	39.60
CENet-MSE w/o MD	7.50	14.20	29.20	38.40
CENet-KL w/o MD	7.90	13.40	28.70	37.40

where different colored dots represent different identities. It can be observed that the sample features of different individuals in the region represented by the blue dashed line are difficult to distinguish. In contrast, CENet w/o MD demonstrates improved inter-class separation and intra-class cohesion, enhancing the overall feature distribution, as shown in Figure 6 (b). This indicates the effectiveness of the proposed network. Furthermore, with the introduction of multi-domain learning, the intra-class compactness is further enhanced, leading to improved discriminability of hard sam-

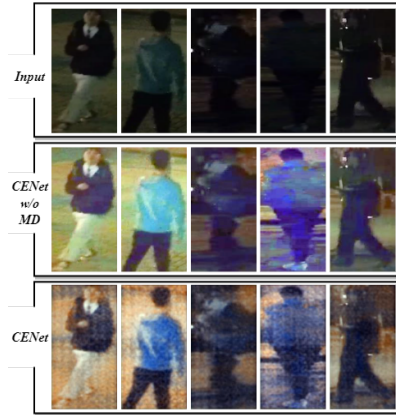


Figure 5. Examples of relighting image under different models

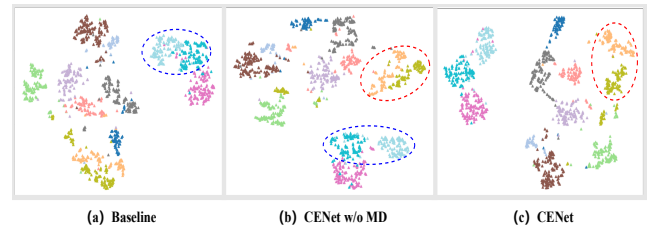


Figure 6. Visualization analysis based on t-SNE technique

ples, as shown in the red dashed region in Figure 6 (c). This confirms the effectiveness of multi-domain learning.

5. Conclusion

In this paper, we presents a novel solution for person ReID in nighttime scenes. By employing a parallel network architecture, we simultaneously perform image relighting and person ReID, mitigating the impact of relighting image quality on the ReID task. We design multi-level feature interaction based on parameter sharing and feature distillation to collaborative modeling two tasks. Furthermore, we propose that multi-domain learning helps enhance feature representation and improve model performance. In future, we plan to explore unsupervised learning schemes for night-

time ReID, allowing to leverage larger-scale unlabeled real nighttime data and further improving performance.

References

- [1] Qiang Chen, Philippe Montesinos, Quan Sen Sun, Peng Ann Heng, et al. Adaptive total variation denoising based on difference curvature. *Image and vision computing*, 28(3):298–306, 2010. 6
- [2] Tianlong Chen, Shaojin Ding, Jingyi Xie, Ye Yuan, Wuyang Chen, Yang Yang, Zhou Ren, and Zhangyang Wang. Abdnnet: Attentive but diverse person re-identification. In *Proceedings of the IEEE International Conference on Computer Vision*, pages 8351–8361, 2019. 1, 7, 8
- [3] François Chollet. Xception: Deep learning with depthwise separable convolutions. In *Proceedings of the IEEE Conference on Computer Vision and Pattern Recognition*, pages 1251–1258, 2017. 6
- [4] Dengxin Dai and Luc Van Gool. Dark model adaptation: Semantic image segmentation from daytime to nighttime. In *Proceedings of the IEEE International Conference on Intelligent Transportation Systems*, pages 3819–3824, 2018. 4
- [5] Navneet Dalal and Bill Triggs. Histograms of oriented gradients for human detection. In *Proceedings of the IEEE Conference on Computer Vision and Pattern Recognition*, pages 886–893, 2005. 3
- [6] Alexey Dosovitskiy, Lucas Beyer, Alexander Kolesnikov, Dirk Weissenborn, Xiaohua Zhai, Thomas Unterthiner, Mostafa Dehghani, Matthias Minderer, Georg Heigold, Sylvain Gelly, et al. An image is worth 16x16 words: Transformers for image recognition at scale. *arXiv preprint arXiv:2010.11929*, 2020. 3, 4
- [7] Zan Gao, Lishuai Gao, Hua Zhang, Zhiyong Cheng, Richang Hong, and Shengyong Chen. Dcr: A unified framework for holistic/partial person reid. *IEEE Transactions on Multimedia*, 23:3332–3345, 2020. 1
- [8] Chunle Guo, Chongyi Li, Jichang Guo, Chen Change Loy, Junhui Hou, Sam Kwong, and Runmin Cong. Zero-reference deep curve estimation for low-light image enhancement. In *Proceedings of the IEEE Conference on Computer Vision and Pattern Recognition*, pages 1780–1789, 2020. 2, 3
- [9] Shuting He, Hao Luo, Pichao Wang, Fan Wang, Hao Li, and Wei Jiang. Transreid: Transformer-based object re-identification. In *Proceedings of the IEEE International Conference on Computer Vision*, pages 14993–15002, 2021. 1, 2, 3, 4, 6, 7, 8
- [10] Yukun Huang, Zhengjun Zha, Xueyang Fu, and Wei Zhang. Illumination-invariant person re-identification. In *Proceedings of the ACM International Conference on Multimedia*, page 365–373, 2019. 2
- [11] Yukun Huang, Zhengjun Zha, Xueyang Fu, Richang Hong, and Liandeng Li. Real-world person re-identification via degradation invariance learning. In *Proceedings of the IEEE Conference on Computer Vision and Pattern Recognition*, pages 14072–14082, 2020. 2
- [12] Daniel J Jobson, Zia-ur Rahman, and Glenn A Woodell. Properties and performance of a center/surround retinex. *IEEE transactions on image processing*, 6(3):451–462, 1997. 3
- [13] Yeong-Taeg Kim. Contrast enhancement using brightness preserving bi-histogram equalization. *IEEE Transactions on Consumer Electronics*, 43(1):1–8, 1997.
- [14] Edwin H Land. The retinex theory of color vision. *Scientific american*, 237(6):108–129, 1977. 3
- [15] Chongyi Li, Chunle Guo, and Chen Change Loy. Learning to enhance low-light image via zero-reference deep curve estimation. *IEEE Transactions on Pattern Analysis and Machine Intelligence*, 44(8):4225–4238, 2021. 2, 3
- [16] Diangang Li, Xing Wei, Xiaopeng Hong, and Yihong Gong. Infrared-visible cross-modal person re-identification with an x modality. In *Proceedings of the AAAI Conference on Artificial Intelligence*, pages 4610–4617, 2020. 2
- [17] Hongchao Li, Chenglong Li, Xianpeng Zhu, Aihua Zheng, and Bin Luo. Multi-spectral vehicle re-identification: A challenge. In *Proceedings of the AAAI Conference on Artificial Intelligence*, pages 11345–11353, 2020. 8
- [18] Andong Lu, Zhang Zhang, Yan Huang, Yifan Zhang, Chenglong Li, Jin Tang, and Liang Wang. Illumination distillation framework for nighttime person re-identification and a new benchmark. *IEEE Transactions on Multimedia*, pages 1–14, 2023. 1, 2, 4, 6, 7, 8
- [19] Hao Luo, Wei Jiang, Youzhi Gu, Fuxu Liu, Xingyu Liao, Shenqi Lai, and Jianyang Gu. A strong baseline and batch normalization neck for deep person re-identification. *IEEE Transactions on Multimedia*, 22(10):2597–2609, 2019. 1, 7, 8
- [20] Dat Tien Nguyen, Hyung Gil Hong, Ki Wan Kim, and Kang Ryoung Park. Person recognition system based on a combination of body images from visible light and thermal cameras. *Sensors*, 17(3):605, 2017. 2
- [21] Etta D Pisano, Shuquan Zong, Bradley M Hemminger, Marla DeLuca, R Eugene Johnston, Keith Muller, M Patricia Braeuning, and Stephen M Pizer. Contrast limited adaptive histogram equalization image processing to improve the detection of simulated spiculations in dense mammograms. *Journal of Digital imaging*, 11:193–200, 1998. 3
- [22] Stephen M Pizer, E Philip Amburn, John D Austin, Robert Cromartie, Ari Geselowitz, Trey Greer, Bart ter Haar Romeny, John B Zimmerman, and Karel Zuiderveld. Adaptive histogram equalization and its variations. *Computer vision, graphics, and image processing*, 39(3):355–368, 1987. 3
- [23] Yifan Sun, Liang Zheng, Yi Yang, Qi Tian, and Shengjin Wang. Beyond part models: Person retrieval with refined part pooling (and a strong convolutional baseline). In *Proceedings of the European Conference on Computer Vision*, pages 501–518, 2018. 7, 8
- [24] Laurens Van der Maaten and Geoffrey Hinton. Visualizing data using t-sne. *Journal of machine learning research*, 9(11), 2008. 7
- [25] Guan-An Wang, Tianzhu Zhang, Yang Yang, Jian Cheng, Jianlong Chang, Xu Liang, and Zeng-Guang Hou. Cross-modality paired-images generation for rgb-infrared person re-identification. In *Proceedings of the AAAI Conference on Artificial Intelligence*, pages 12144–12151, 2020. 2

- [26] Zi Wang, Chenglong Li, Aihua Zheng, Ran He, and Jin Tang. Interact, embed, and enlarge: Boosting modality-specific representations for multi-modal person re-identification. In *Proceedings of the AAAI Conference on Artificial Intelligence*, pages 2633–2641, 2022. 7, 8
- [27] Chen Wei, Wenjing Wang, Wenhan Yang, and Jiaying Liu. Deep retinex decomposition for low-light enhancement. *arXiv preprint arXiv:1808.04560*, 2018. 3, 6
- [28] Longhui Wei, Shiliang Zhang, Wen Gao, and Qi Tian. Person transfer gan to bridge domain gap for person re-identification. *Proceedings of the IEEE Conference on Computer Vision and Pattern Recognition*, pages 79–88, 2018. 2, 5, 7
- [29] Ancong Wu, Wei-Shi Zheng, Hongxing Yu, Shaogang Gong, and Jianhuang Lai. Rgb-infrared cross-modality person re-identification. In *Proceedings of the IEEE International Conference on Computer Vision*, pages 5380–5389, 2017. 2
- [30] Mang Ye, Weijian Ruan, Bo Du, and Mike Zheng Shou. Channel augmented joint learning for visible-infrared recognition. In *Proceedings of the International Conference on Computer Vision*, pages 13567–13576, 2021. 2
- [31] Mang Ye, Jianbing Shen, Gaojie Lin, Tao Xiang, Ling Shao, and Steven C. H. Hoi. Deep learning for person re-identification: A survey and outlook. *IEEE Transactions on Pattern Analysis and Machine Intelligence*, 44(6):2872–2893, 2021. 1, 7, 8
- [32] Mang Ye, Jianbing Shen, and Ling Shao. Visible-infrared person re-identification via homogeneous augmented tri-modal learning. *IEEE Transactions on Information Forensics and Security*, 16:728–739, 2021. 2
- [33] Mang Ye, Cuiqun Chen, Jianbing Shen, and Ling Shao. Dynamic tri-level relation mining with attentive graph for visible infrared re-identification. *IEEE Transactions on Information Forensics and Security*, 17:386–398, 2022. 1, 2
- [34] Mang Ye, He Li, Bo Du, Jianbing Shen, Ling Shao, and Steven C. H. Hoi. Collaborative refining for person re-identification with label noise. *IEEE Transactions on Image Processing*, 31:379–391, 2022.
- [35] Mang Ye, Jianbing Shen, Xu Zhang, Pong C. Yuen, and Shih-Fu Chang. Augmentation invariant and instance spreading feature for softmax embedding. *IEEE Transactions on Pattern Analysis and Machine Intelligence*, 44(2):924–939, 2022. 1
- [36] Jian’an Zhang, Yuan Yuan, and Qi Wang. Night person re-identification and a benchmark. *IEEE Access*, 7:95496–95504, 2019. 1, 2, 4
- [37] Yu Zhang, Xiaoguang Di, Bin Zhang, and Chunhui Wang. Self-supervised image enhancement network: Training with low light images only. *arXiv preprint arXiv:2002.11300*, 2020. 2, 3, 6
- [38] Yonghua Zhang, Xiaojie Guo, Jiayi Ma, Wei Liu, and Jiawan Zhang. Beyond brightening low-light images. *International Journal of Computer Vision*, 129:1013–1037, 2021. 3
- [39] Yiyuan Zhang, Yuhao Kang, Sanyuan Zhao, and Jianbing Shen. Dual-semantic consistency learning for visible-infrared person re-identification. *IEEE Transactions on Information Forensics and Security*, pages 1–1, 2022. 2
- [40] Ziyue Zhang, Richard Y. D. Xu, Shuai Jiang, Yang Li, Congzhenhao Huang, and Chen Deng. Illumination adaptive person reid based on teacher-student model and adversarial training. In *Proceedings of the International Conference on Image Processing*, pages 2321–2325, 2020. 2
- [41] Aihua Zheng, Zi Wang, Zihan Chen, Chenglong Li, and Jin Tang. Robust multi-modality person re-identification. In *Proceedings of the AAAI Conference on Artificial Intelligence*, pages 3529–3537, 2021. 7, 8
- [42] Liang Zheng, Liyue Shen, Lu Tian, Shengjin Wang, Jingdong Wang, and Qi Tian. Scalable person re-identification: A benchmark. In *Proceedings of the IEEE International Conference on Computer Vision*, pages 1116–1124, 2015. 2, 5, 7
- [43] Zhedong Zheng, Liang Zheng, and Yi Yang. A discriminatively learned cnn embedding for person reidentification. *ACM transactions on multimedia computing, communications, and applications*, 14(1):1–20, 2017. 7, 8